

# How Sensitive Are Weak Lensing Statistics to Dark Energy Content?

Dipak Munshi<sup>1,2</sup>, and Yun Wang<sup>3</sup>

<sup>1</sup>*Institute of Astronomy, Madingley Road, Cambridge, CB3 OHA, United Kingdom*

<sup>2</sup>*Astrophysics Group, Cavendish Laboratory, Madingley Road, Cambridge, CB3 OHE, United Kingdom*

<sup>3</sup>*Department of Physics & Astronomy, University of Oklahoma, Norman, OK 73019 USA.*

*munshi@ast.cam.ac.uk, wang@mail.nhn.ou.edu*

## ABSTRACT

Future weak lensing surveys will directly probe the clustering of dark matter, in addition to providing a test for various cosmological models. Recent studies have provided us with the tools which can be used to construct the complete probability distribution function for convergence fields. It is also possible to construct the bias associated with the hot-spots in convergence maps. These techniques can be used in both the quasi-linear and the highly nonlinear regimes using various well developed numerical methods. We use these results here to study the weak lensing statistics of cosmological models with dark energy. We study how well various classes of dark energy models can be distinguished from models with a cosmological constant. We find that the ratio of the square root of the variance of convergence is complementary to the convergence skewness  $S_3$  in probing dark energy equation of state; it can be used to predict the expected difference in weak lensing statistics between various dark energy models, and for choosing optimized smoothing angles to constrain a given class of dark energy models. Our results should be useful for probing dark energy using future weak lensing data with high statistics from galaxy weak lensing surveys and supernova pencil beam surveys.

*Subject headings:* Cosmology: theory – weak lensing – Methods: analytical – Methods: statistical – Methods: numerical

## 1. Introduction

Recent cosmological observations favor an accelerating universe (Garnavich et al. 1998a; Riess et al. 1998; Perlmutter et al. 1999). This implies the existence of energy of unknown

nature (dark energy), which has negative pressure. Current data are consistent with dark energy being a non-zero cosmological constant (see for example, Wang & Garnavich 2001; Bean & Melchiorri 2002). Many other alternative dark energy candidates have been considered, and are consistent with data as well. For example, quintessence, k-essence, spintessence, etc. (Peebles & Ratra 1988; Frieman et al. 1995; Caldwell, Dave, & Steinhardt 1998; Garnavich et al. 1998b; White 1998; Efstathiou 1999; Steinhardt, Wang, & Zlatev 1999; Podariu & Ratra 2000; Sahni & Wang 2000; Sahni & Starobinsky 2000; Saini et al. 2000; Waga & Frieman 2000; Huterer & Turner 2001; Ng & Wiltshire 2001; Podariu, Nugent, & Ratra 2001; Weller & Albrecht 2001)

Different dark energy models can be conveniently classified according to the equation of state of the dark energy component,  $w_X$ . For example, for quintessence models,  $dw_X/dz > 0$ , while for k-essence models,  $dw_X/dz < 0$ . There are many complimentary probes of dark energy. These include, the distance-redshift relations of cosmological standard candles, Cosmic Microwave Background Anisotropy, volume-redshift test using galaxy counts, the evolution of galaxy clustering, weak lensing, etc. These different methods to probe dark energy are complimentary to each other, and can provide important consistency checks, due to the different sources of systematics in each method (for example, see Kujat et al. 2002).

Weak lensing surveys (Bacon, Refregier & Ellis 2000; Van Waerbeke et al. 2000; Wittman et al. 2000; Maoli et al. 2001; Van Waerbeke et al. 2001; Wilson, Kaiser, & Luppino 2001; Bacon et al. 2002; Hoekstra et al. 2002; Refregier, Rhodes & Groth 2002), currently underway and more proposed in the near future, are well suited to studying the dark energy equation of state. Weak lensing directly probes the gravitational clustering and the background cosmology. Many recent studies, both theoretical and numerical, have analyzed these possibilities. Observational teams have already reported first detections of cosmic shear. On theoretical front progress has been made in modeling the statistics using both perturbative calculations which are valid for large smoothing angles and also using the well motivated hierarchical ansatz which is valid for small smoothing angles. Numerical studies carried out so far uses ray shooting experiments and are quite useful in testing analytical calculations.

In an earlier study on probing quintessence using weak lensing, Hui (1999) concluded that the large scale convergence skewness can directly provide a constraint for  $w_X$ , the equation of state of dark energy. Similarly, Huterer studied the use of weak lensing convergence power spectrum and three-point statistics to constrain dark energy models. Both of these papers are useful in utilizing large weak lensing surveys of galaxies to constrain dark energy.

In this paper we construct the complete probability distribution function of convergence to study the effects of dark energy. Our results apply to the weak lensing of both galaxies

(on large angular scales) and type Ia supernovae (on small angular scales). We compare two classes of dark energy models (one with effective constant equation of state  $w_X$ , the other with time-varying  $w_X$ ) against that of a  $\Lambda$  dominated universe.

The technique we use in this paper has been tested in detail using N-body calculations. Analytical results are obtained for large smoothing angles using the perturbative calculations, and for small smoothing angles using the hierarchical ansatz. We focus on both the one-point probability distribution function and the bias associated with convergence maps in the quasi-linear and the highly nonlinear regimes. Our studies are quite complementary to the studies done using a Fisher matrix analysis for the recovery of power spectra from observations. While such studies are well suited for recovering the nonlinear matter power spectra; the study of the probability distribution function and the bias will give us a direct probe of non-Gaussianity developed through gravitational clustering.

The paper is organized as follows. In Section 2 we give the definition of some basic equations for reference, and identify the dark energy models studied in this paper. Section 3 discusses the weak lensing statistics of dark energy models. Section 4 contains discussions and a summary.

## 2. Notation

The weak lensing convergence,  $\kappa$ , maps the distribution of projected density fields, and its statistics is directly related to that of the underlying matter distribution. We write

$$\kappa(\theta_0) = \int_0^{\chi_s} d\chi \omega(\chi) \delta(r(\chi)\theta_0, \chi), \quad (1)$$

where  $r(\chi)$  is the angular diameter distance and  $\omega(\chi)$  is the weight function associated with the source distribution. The observer is placed at  $\chi = 0$ , and the sources (which for simplicity we assume are all at the same redshift) are placed at  $\chi_s$ .  $\chi$  is given by

$$\chi(z) = cH_0^{-1} \int_0^z dz' [\Omega_m(1+z')^3 + \Omega_k(1+z')^2 + \Omega_X f(z)]^{-1/2} \quad (2)$$

where the  $\Omega$ 's denote the fraction of critical density in various components.  $\Omega_X$  denotes the dark energy component, and  $\Omega_k = 1 - \Omega_m - \Omega_X$ . The function  $f(z)$  parametrizes the time-dependence of the dark energy density, and  $f(z=0) = 1$ . For dark energy with constant equation of state,  $w_X = p_X/\rho_X = constant$ ,  $f(z) = (1+z)^{3(1+w_X)}$ . The limiting case with  $w_X = -1$  [i.e.,  $f(z) = 1$ ] corresponds to a cosmological constant. Note that to

obtain accelerated expansion of the universe, we need  $\rho + 3p < 0$ , which implies  $w_X < -1/3$  for a power law dark energy density  $f(z)$ . In general, the dark energy equation of state,  $w_X(z)$ , can be written in terms of the dimensionless dark energy density,  $f(z)$ ,  $w_X(z) = \frac{1}{3}(1+z)f'(z)/f(z) - 1$ , for dark energy density or equation of state with arbitrary time dependence. (Wang & Garnavich 2001)

We study two classes of dark energy models. The first class contains dark energy models with effective constant equation of state,  $w_X = -1/3, -2/3, -1$  ( $\Lambda$ CDM), and  $-1.9$ . If dark energy arises from classical fields, it must satisfy the weak energy condition, which requires that  $w_X > -1$ . The weak energy condition violating toy model,  $w_X = -1.9$ , is motivated by quantum gravity models of inflation in which quantum effects lead to the violation of the weak energy condition (Onemli & Woodard 2002). The second class contains two dark energy toy models with linear time-varying equations of state,  $w_X = w_q(z) = -1 + z$  and  $-1 + 2z/3$ . These are motivated by quintessence models which have  $w_X$  that effectively increases with  $z$ . All the models have  $\Omega_m = 0.3$ ,  $\Omega_X = 0.7$ ,  $h = 0.7$ ,  $n_S = 1$  (power law index of the primordial power spectrum), and  $\sigma_8 = 0.8$ . We normalize the nonlinear power spectrum to  $\sigma_8$ . Table 1 lists these dark energy models.

Table 1  
Dark Energy Models

| Model          | $w_X(z)$            |
|----------------|---------------------|
| $\Lambda$ CDM  | -1                  |
| constant $w_X$ | $-1/3, -2/3, -1.9$  |
| $w_q(z)$       | $-1 + 2z/3, -1 + z$ |

The two classes of dark energy models are compared with the fiducial  $\Lambda$ CDM model to quantify the variation in various statistics of convergence maps.

### 3. Statistics of Weak Lensing in Dark Energy Models

To compute the statistics of weak lensing convergence field, we need to relate it to the statistics of three dimensional density field of underlying matter distribution. In recent studies such analysis has been done extensively. We use such a formalism to explore the weak lensing statistics for the dark energy cosmologies. For large smoothing angles we use the perturbative calculations and for small smoothing angles we use the well motivated hierarchical ansatz to compute the relevant quantities.

### 3.1. Evolution of the Matter Power Spectrum

We compute the matter power spectrum using the scaling ansatz of Hamilton et al. (1991), which was later extended by various authors [see e.g. Peacock & Dodds (1996)]. This ansatz essentially consists of postulating that  $4\pi k^3 P(k) = f[4\pi k_l^3 P_l(k_l)]$ , where  $P(k)$  is the nonlinear power spectrum and  $P_l$  is the linear power spectrum, and the function  $f$  in general will depend on the initial power spectrum. The linear power spectrum is evaluated at a different wave number,  $k_l = (1 + 4\pi k^3 P(k))^{-1/3} k$ , hence the mapping is non-local in nature. The cosmological model enters through the linear growth function  $g(z)$ , so that  $P_l(k, z) = [g(z)/(1 + z)]^2 P_l(k, z = 0)$ . The linear growth function is given by:

$$g(z) = \frac{\delta(z, \Omega_m, \Omega_\Lambda)}{\delta(z, \Omega_m = 1)} = \frac{5}{2} \Omega_m (1 + z) E(z) \int_z^\infty dz' \frac{(1 + z')}{[E(z')]^3}, \quad (3)$$

Where

$$E(z) \equiv \sqrt{\Omega_m (1 + z)^3 + \Omega_k (1 + z)^2 + \Omega_X f(z)} \quad (4)$$

We compute the linear growth function by direct integration [for more on power spectrum evolution in quintessence models see (Benabed & Bernardeau 2001)].

Our method enforces stable clustering in the nonlinear regime and assumes the hierarchical ansatz (which is tested by numerous numerical simulations), therefore we are able to predict the higher order correlation functions (Davis & Peebles 1977, Groth & Peebles 1977, Fry & Peebles 1978) and (their Fourier transforms or) the multi-spectrum correctly. Combining these with the powerful technique of the generating function we can construct the complete probability distribution function and the bias associated with convergence maps.

### 3.2. Convergence Probability Distribution Function

Perturbative calculations depend on the expansion of the convergence field  $\kappa(\theta_0)$  for smoothing angle  $\theta_0$  in terms of perturbative expansion of the density field  $\delta$ . Such an analysis can be performed in an order by order manner,

$$\kappa^{(1)}(\theta_0) + \kappa^{(2)}(\theta_0) + \dots = \int_0^{\chi_s} d\chi \omega(\chi) [\delta^{(1)}(r(\chi)\theta_0) + \delta^{(1)}(r(\chi)\theta_0) + \dots] \quad (5)$$

where  $\delta^{(i)}$  and  $\kappa^{(i)}$  correspond to the  $i$ -th order perturbative expansion,  $i = 1$  being the linear order. In the perturbative regime at tree level (Fry 1984; Bernardeau 1992, 1994; Bernardeau & Schaeffer 1992), it is possible to introduce vertex generating function  $G(\tau)$  which will encode the tree level contribution from all orders. The smoothing using a top-hat filter function can be incorporated in the generating function formalism and then the generating function can be written in terms of the generating function of the unsmoothed case. All statistical quantities including probability distribution functions can be constructed once we have solved for the tree-level generating functions (Bernardeau 1992, 1994). We write

$$G(\tau) = \left(1 - \frac{\tau}{\kappa_a}\right)^{-\kappa_a}; \quad G_s^{PT}(\tau) = G^{PT} \left[ \tau \frac{\sigma(R_0(1 + G^{PT}(\tau))^{1/2})}{\sigma(R_0)} \right] \quad (6)$$

The parameter  $\kappa_a$  can be determined from the dynamical equation governing the evolution of perturbations in the quasi-linear regime, and it is given by  $\kappa_a = \frac{\sqrt{13}-1}{2}$ . The variance at a length scale  $\sigma(R_0) = R_0^{-(n+3)/2}$ , where a local power law spectrum index  $n$  is used to evaluate the generating function. The generating function is now used to compute the probability distribution function at a particular smoothing scale.

In the highly nonlinear regime (Balian & Schaeffer 1989, Davis & Peebles 1977, Groth & Peebles 1977, Szapudi & Szalay 1993, Scoccimarro & Frieman 1999, Munshi et al. 1999c), the perturbative series starts to diverge and the usual perturbative calculations are replaced by the hierarchical ansatz for higher order correlation functions, which can be built from two-point correlation functions. The amplitude of various contributions can be constructed from the knowledge of the generating function. It was found from analytical reasoning and numerical experimentation that the generating function in the highly nonlinear regime retains exactly the same form as in the quasi-linear regime; however, the value of  $\kappa_a$  is changed (Beranrdeau 1992) – it is now treated as a free parameter (Colombi et al. 1995, Munshi et al. 1999a,b). It is customary to use a different parameter  $\omega$  that is easy to evaluate from numerical simulations,  $\kappa_a = \frac{2\omega}{(1-\omega)}$ . It was found that  $\omega = .3$  reproduces various statistics in the nonlinear regime quite well (Colombi et al. 1997, Colombi, Bouchet, Schaeffer 1995, Munshi et al. 1999d). To compute the probability distribution function, one has to compute the void probability function  $\phi(y)$ , which acts as a generating function for normalized cumulants or  $S_N$  parameters and can be expressed in terms of the function  $G(\tau)$  as (Balian & Schaeffer 1989):

$$\begin{aligned} \phi(y) &= yG(\tau) - \frac{1}{2}y\tau\frac{d}{d\tau}G(\tau) \\ \tau &= -y\frac{d}{d\tau}G(\tau). \end{aligned} \quad (7)$$

Finally the probability distribution function can now be written as (Balian & Schaeffer 1989):

$$P(\delta) = \int_{-i\infty}^{i\infty} \frac{dy}{2\pi i} \exp \left[ \frac{(1+\delta)y - \phi(y)}{\bar{\xi}_2} \right] \quad (8)$$

In recent studies it was found that in both the quasi-linear and the highly nonlinear regimes, it is possible to introduce a reduced convergence field (Munshi & Jain 2000, Munshi 2002),  $\eta = \frac{\kappa - \kappa_{min}}{-\kappa_{min}}$ , which to a very good approximation follows the same statistics as  $1 + \delta$ . In the quasi-linear regime it follows the smoothed projected density, and in the highly nonlinear regime it simply follows the 3D statistics of the density field.<sup>1</sup>

The variance of  $\eta$  is given by (Valageas 2000a; Valageas 2000b)

$$\xi_\eta = \int_0^{\chi_s} d\chi \left( \frac{w}{F_s} \right)^2 I_\mu(\chi), \quad (9)$$

with

$$\begin{aligned} w(\chi, \chi_s) &= \frac{H_0^2}{c^2} \frac{\mathcal{D}(\chi) \mathcal{D}(\chi_s - \chi)}{\mathcal{D}(\chi_s)} (1 + z), & \mathcal{D}(\chi) &= \frac{c H_0^{-1}}{\sqrt{|\Omega_k|}} \text{sinn} \left( \sqrt{|\Omega_k|} \chi \right) \\ F_s &= \int_0^{\chi_s} d\chi w(\chi, \chi_s), & I_\mu(z) &= \pi \int_0^\infty \frac{dk}{k} \frac{\Delta^2(k, z)}{k} W^2(\mathcal{D}k\theta_0), \end{aligned} \quad (10)$$

where “sinn” is defined as  $\sinh$  if  $\Omega_k > 0$ , and  $\sin$  if  $\Omega_k < 0$ . If  $\Omega_k = 0$ , the sinn and  $\Omega_k$ ’s disappear.  $\Delta^2(k, z) = 4\pi k^3 P(k, z)$ ,  $k$  is the wavenumber,  $P(k, z)$  is the matter power spectrum, The window function  $W(\mathcal{D}k\theta_0) = 2J_1(\mathcal{D}k\theta_0)/(\mathcal{D}k\theta_0)$  for smoothing angle  $\theta_0$ . Here  $J_1$  is the Bessel function of order 1. Note that the clustering of the dark energy field would lead to an increase in the transfer function on very large scales. Huterer (2002) has shown that the clustering of the dark energy field can be neglected on the scales relevant to weak lensing surveys.

Fig.1 shows  $-\kappa_{min}$  and  $\sqrt{\xi_\eta}$ , and Figs. 2 & 3 show the pdf for the two classes of dark energy models listed in Table 1.

---

<sup>1</sup>It was recently shown by Munshi (2002) that analytical results obtained by direct perturbative calculations can also be obtained by using a functional fit obtained from assuming a log-normal evolution of local correlated density field. This method was also found not only to work for one point probability distribution function but also for bias associated with convergence maps.

### 3.3. Bias Associated with Convergence Maps

Assuming a correlation function hierarchy guarantees that we have a two-point probability distribution function  $P(\kappa_1, \kappa_2)$  which can be factorized as follows (Munshi 2001),

$$P(\kappa_1, \kappa_2) d\kappa_1 d\kappa_2 = P(\kappa_1)P(\kappa_2) [1 + b(\kappa_1)\xi_{12}^\kappa b(\kappa_2)] d\kappa_1 d\kappa_2. \quad (11)$$

The function  $\xi_{12}^\kappa$  is the two point correlation function corresponding to convergence maps. The function  $b(\kappa)$  is the bias associated with the convergence maps, and can be shown to be related to the bias associated with overdense regions,  $b(1+\delta)$  (Munshi 2001). The perturbative calculations also produce similar results, although the nature of the bias function  $b(\kappa)$  changes from one regime to another. As was the case for one point normalized moments, whose generating function was related to the one point probability distribution function, the generating functions for two-point collapsed higher order correlation functions, also known as cumulant correlators, are also related to the bias function in a very similar manner. We write

$$P(\delta)b(\delta) = \int_{-i\infty}^{i\infty} \frac{dy}{2\pi i} \tau \exp \left[ \frac{(1+\delta)y - \phi(y)}{\bar{\xi}_2} \right], \quad (12)$$

where  $\tau$  is a generating function for the cumulant correlators. However, it turns out that the differential bias, as we have written down above, is difficult to estimate from numerical data. Therefore we work with the cumulative bias, which is the bias associated with points where convergence maps cross a particular threshold (Munshi 2001). Previous studies against numerical simulations showed that the bias function describes the numerical results quite accurately. It was shown in earlier studies that  $b(\kappa) = \frac{b(1+\delta)}{\kappa_{min}}$ .

Figures 4 & 5 show the cumulative bias for the two classes of dark energy models indicated in Figure 1. Clearly, the cumulative bias of convergence is complementary to the convergence pdf in probing the non-Gaussianity of gravitational clustering and constraining dark energy models.

### 3.4. A New Indicator for Deviations from the $\Lambda$ CDM model

We find that the deviations of dark energy models from the fiducial  $\Lambda$ CDM model can be quantified with a single parameter

$$1 + \epsilon \equiv \frac{\sqrt{\xi_\kappa(\text{XCDM})}}{\sqrt{\xi_\kappa(\Lambda\text{CDM})}} = \frac{\kappa_{\min}(\text{XCDM}) \sqrt{\xi_\eta(\text{XCDM})}}{\kappa_{\min}(\Lambda\text{CDM}) \sqrt{\xi_\eta(\Lambda\text{CDM})}}, \quad (13)$$

where XCDM represents an arbitrary dark energy model. Figure 6 shows the indicator  $1 + \epsilon$  for the two classes of dark energy models studied in this paper, for smoothing angle  $\theta_0 = 1'$  and  $15'$ .

Comparison of Fig.6 and Figs.2-3 shows that the more the pdf of the dark energy model differs from that of the fiducial  $\Lambda\text{CDM}$  model, the more the indicator  $1 + \epsilon$  deviates from one. This indicates that the pdf is primarily determined by its variance, which is consistent with the finding of the existence of a universal probability distribution function (in terms of the scaled convergence  $\eta$ ) for weak lensing amplification by Wang, Holz, & Munshi (2002).

It is useful to compare our new indicator with the convergence skewness  $S_3$  (Hui 1999) for the same models. Figure 7 shows  $S_3$  for the same models as in Figure 6, with the same line and arrow types. We have computed the convergence skewness  $S_3$  using Hyper-Extended Perturbation theory in the nonlinear regime (small smoothing angular scales), and perturbative results are adopted for the quasi-linear regime (larger smoothing angular scales). While  $S_3$ , as an indicator, mainly encodes the information about non-Gaussianity, the indicator we have proposed is directly related to the variance and is more sensitive to the projected density power spectrum.

Our new weak lensing pdf shape indicator,  $1 + \epsilon$ , is complementary to  $S_3$  in constraining the dark energy equation of state. The indicator,  $1 + \epsilon$ , is sensitive to smoothing angle  $\theta_0$ , while  $S_3$  is not very sensitive to  $\theta_0$  at small angular scales. Feasible future supernova surveys can yield a large number of type Ia supernovae out to redshift  $z = 1$  and beyond (Wang 2000, SNAP<sup>2</sup>). It may be possible to directly measure the weak lensing pdf with sufficiently high statistics (Metcalf & Silk 1999; Seljak & Holz 1999); this would allow us to utilize the pdf with different smoothing angles to probe different ranges of constant  $w_X$  models, and the variation of  $w_X$  with  $z$ .

#### 4. Discussions and Summary

We have analyzed weak lensing statistics for two classes of dark energy cosmological models. One class of dark energy models have effective constant equation of state  $w_X$ , while the other have linear time-varying  $w_X(z)$  inspired by quintessence models. The weak lensing

---

<sup>2</sup>See <http://snap.lbl.gov>.

statistics of these dark energy models are compared with that of a  $\Lambda$ CDM model.

It has been shown that in directly using the distance-redshift relations of type Ia supernovae to probe dark energy, it is optimal to measure the dark energy density,  $\rho_X(z) = \rho_X(0) f(z)$ , instead of the dark energy equation of state,  $w_X(z)$ . (Wang & Garnavich 2001; Wang & Lovelace 2001; Tegmark 2001) In this paper, for convenience and illustration, we have used  $w_X$  to classify various models.

Note that we have considered a dark energy toy model which violates the weak energy condition, as similar models could arise from quantum effects in quantum gravity models of inflation (Onemli & Woodard 2002). Also, we have only considered dark energy models with linear time-varying  $w_X(z)$ , although dark energy models with much more complicated time dependence in  $w_X(z)$  have been proposed (see for example, Bassett et al. 2002). This is because it is extremely difficult to extract the time dependence of  $w_X(z)$ , even if it were a simple linear function of the redshift  $z$ , from observational data (for example, see Maor et al. 2001; Barger & Marfatia 2001; Wang & Garnavich 2001; Kujat et al. 2002; Maor et al. 2002).

We have studied the statistics of the cosmic convergence field via various diagnostics including the one point probability distribution functions and the bias associated with convergence “hot spots”. The analysis was done for both the quasi-linear scales where perturbative calculations are valid and also for very small angular scales where hierarchical ansatz is generally used to quantify the statistical distributions. Following earlier studies we introduce a quantity  $\kappa_{min}$  which can help us to write the observed convergence field in terms of a reduced convergence field which in turn represents directly the statistics of density distribution. For large smoothing angles, perturbation theory predicts this quantity  $\eta$  to trace the projected density field, and on small angular scales it traces the nonlinear density field in three dimensions. The lower order moments corresponding to various cosmologies have already been investigated in detail and our studies complement these results. Also we have used top-hat window functions, but Bernardeau & Valageas (2000) have shown how to generalize similar calculations in terms of aperture mass using compensated filters.

We have identified a new weak lensing pdf shape indicator,  $1 + \epsilon \propto \sqrt{\xi_\kappa} = \kappa_{min} \sqrt{\xi_\eta}$ , which can be used to predict the expected difference in weak lensing statistics between various dark energy models, and for choosing optimized smoothing angles to constrain a given class of dark energy models. For example, small smoothing angles are favored for constraining dark energy models with  $w_X < -1$ .

We have computed the convergence skewness  $S_3$  for the dark energy models considered in this paper. We find that the new weak lensing pdf shape indicator,  $1 + \epsilon$ , is complementary

to  $S_3$  in probing dark energy equation of state.

With high statistics data from future weak lensing surveys of galaxies and supernova pencil beam surveys (Wang 2001; SNAP), weak lensing can be a useful tool in differentiating different dark energy models.

DM was supported by PPARC grant RG28936, and YW was supported in part by NSF CAREER grant AST-0094335. DM would like to thank Alexandre Refregier for many useful discussion, and Francis Bernardeau for making a copy of his code to compute the pdf and bias available to us.

## REFERENCES

Bacon, D.J.; Refregier, A.R.; Ellis, R.S. 2000, MNRAS, 318, 625

Bacon, D.J.; Massey, R.; Refregier, A.R.; Ellis, R.S. 2002, astro-ph/0203134, submitted to MNRAS

Benabed,K., Bernardeau, F., Phys.Rev. D64 (2001) 083501

Barger, V., & Marfatia, D. 2001, Phys. Lett. B, 498, 67

Balian R., Schaeffer R., 1989, A& A, 220, 1

Bartelmann, M., Schneider, P., 1991, A& A, 248, 353

Bassett, B. A., Kunz, M., Silk, J., & Ungarelli, C. 2002, astro-ph/0203383

Bean, R., & Melchiorri, A., Phys.Rev. D65 (2002) 041302

Bernardeau, F., 1992, ApJ, 392, 1

Bernardeau, F., 1994, A& A, 291, 697

Bernardeau, F., 1998, A& A, 338, 375

Bernardeau, F., Schaeffer, R., 1992, A& A, 255, 1

Bernardeau, F., van Waerbeke, L., Mellier, Y., 1997, A& A, 322, 1

Bernardeau, F.; Valageas, P. 2000, A & A, 364, 1

Blandford, R.D., Saust, A.B., Brainerd, T.G., Villumsen, J.V., 1991, MNRAS, 251, 600

Boschan, P., Szapudi, I., Szalay, A.S. 1994, ApJS, 93, 65

Caldwell, R.R., Dave, R., Steinhardt, P.J. 1998, Phys. Rev. Lett. 80, 1582

Colombi, S., Bouchet, F.R., Schaeffer, R., 1995, ApJS, 96, 401

Colombi, S., Bernardeau, F., Bouchet, F.R., Hernquist, L., 1997, MNRAS, 287, 241

Davis, M., Peebles, P.J.E., 1977, ApJS, 34, 425

Efstathiou, G. 1999, MNRAS, 310, 842

Frieman, J.A.; Hill, C.T.; Stebbins, A.; & Waga, I. 1995, Phys. Rev. Lett. 75, 2077

Fry, J.N., 1984, ApJ, 279, 499

Fry, J.N., Peebles, P.J.E., 1978, ApJ, 221, 19

Garnavich, P.M. et al. 1998a, ApJ, 493, L53

Garnavich, P.M. et al. 1998b, ApJ, 509, 74

Groth, E., Peebles, P.J.E., 1977, ApJ, 217, 385

Hamilton, A.J.S., Kumar, P., Lu, E., Matthews, A., 1991, ApJ, 374, L1

Hoekstra, H., et al. 2002, ApJ, 572, 55

Hui, L., 1999, ApJ, 519, L9

Huterer, D., & Turner, M. S. 2001, Phys. Rev. D64, 123527

Huterer, D. 2002, Phys. Rev. D65, 063001

Jain, B., Mo H.J., White S.D.M., 1995, MNRAS, 276, L25

Jain, B., Seljak, U., 1997, ApJ, 484, 560

Jain, B., van Waerbeke L., 2000, ApJ, 530, L1

Kaiser, N., 1992, ApJ, 388, 272

Kaiser, N., 1998, ApJ, 498, 26

Kujat, J., Linn, A.M., Scherrer, R.J., Weinberg, D.H. 2002, ApJ, 572, 1-14, 2001

Maoli, R., et al. 2001, A & A, 368, 766

Maor, I., Brustein, R., & Steinhardt, P.J. 2001, Phys. Rev. Lett., 86, 6; Erratum-ibid. 87 (2001) 049901

Maor, I., Brustein, R., McMahon, J., & Steinhardt, P.J. 2002, Phys. Rev. D65 (2002) 123003

Metcalf, R. B., & Silk, J. 1999, ApJ, 519, L1

Munshi, D., Coles, P., Melott, A.L., 1999a, MNRAS, 307, 387

Munshi, D., Coles, P., Melott, A.L., 1999b, MNRAS, 310, 892

Munshi, D., Melott, A.L., Coles, P., 1999c, MNRAS, 311, 149

Munshi, D., Bernardeau, F., Melott, A.L., Schaeffer, R., 1999d, MNRAS, 303, 433

Munshi, D., Coles, P., 2000a, MNRAS, 313, 148

Munshi, D., Coles, P., 2000b, MNRAS, submitted

Munshi, D., Jain, B., 2000, MNRAS, 318, 109

Munshi, D., 2001, MNRAS, 322, 107

Ng, S.C.C., & Wiltshire, D.L. 2001, Phys. Rev. D64, 123519

Onemli, V. K., Woodard, R. P. 2002, gr-qc/0204065.

Peacock, J.A., Dodds, S.J., 1996, MNRAS, 280, L19

Peebles, P. J. E.; & Ratra, B. 1988, ApJ, 325L, 17

Perlmutter, S., et al. 1999, ApJ, 517, 565

Podariu, S., & Ratra, B. 2000, ApJ, 532, 109

Podariu, S., Nugent, P., & Ratra, B. 2001, ApJ, 553, 39

Refregier, A., Rhode, J., & Groth, E., 2002, ApJ, 572, L131

Rhode, J., Refregier, A., Groth, E., 2001, ApJ, 552, L85

Riess, A.G., et al 1998, AJ, 116, 1009

Sahni, V., & Starobinsky, A. 2000, Int. J. Mod. Phys. D, 9, 373

Sahni, V., & Wang, L. 2000, Phys. Rev. D, 62, 103517

Saini, T.; Raychaudhury, S.; Sahni, V.; and Starobinsky, A.A. 2000, Phys. Rev. Lett., 85, 1162

Scoccimarro R., & Frieman J.A. 1999, ApJ, 520, 35

Seljak, U., & Holz, D. E. 1999, A&A, 351, L10

Steinhardt, P.J., Wang, L., & Zlatev, I. 1999, Phys. Rev. D59, 123504

Szapudi, I., Szalay, A.S., 1993, ApJ, 408, 43

Tegmark, M. 2001, astro-ph/0101354

Valageas, P., 2000a, A& A, 354, 767

Valageas, P., 2000b, A& A, 356, 771

Van Waerbeke, L. et al. 2000, A & A, 358, 30

Van Waerbeke, L., et al. 2001, A & A, 374, 757

Waga, I., & Frieman, J.A. 2000, Phys.Rev. D62, 043521

Wang Y., 1999, ApJ, 525, 651

Wang, Y. 2000, ApJ, 531, 676

Wang, Y. & Garnavich, P. 2001, ApJ, 552, 445

Wang, Y. & Lovelace, G. 2001, ApJ, 562, L115

Wang Y., Holz, D.E., & Munshi, D. 2002, ApJ, 572, L15

Weller, J., & Albrecht, A. 2001, astro-ph/0106079

White, M. 1998, ApJ, 506, 495

Wilson, G.; Kaiser, N.; Luppino, G.A. 2001, ApJ, 556, 601

Wittman, D.M, Tyson, J.A., Kirkman, D., Dell'Antonio,I., Bernstein, G., 2000, nature, 405, 143

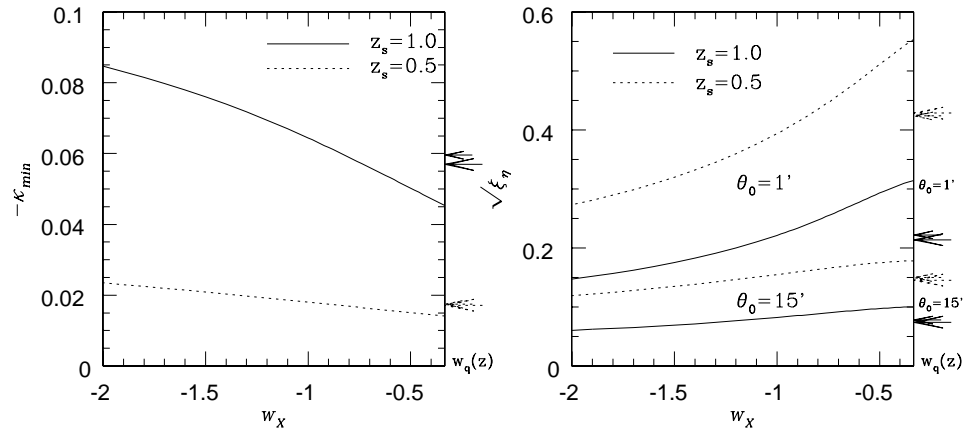


Fig. 1.— The minimum value of the convergence field,  $\kappa_{min}$ , and variance of the scaled convergence  $\eta = 1 + \kappa/|\kappa_{min}|$ ,  $\xi_\eta$ , as functions of constant dark energy equation of state,  $w_X$ , for source redshift  $z_s = 0.5$  and 1.0. The arrows indicate the  $-\kappa_{min}$  and  $\sqrt{\xi_\eta}$  values for dark energy models with time-varying equation of state,  $w_q(z) = -1 + z$  (long arrows) and  $w_q(z) = -1 + 2z/3$  (short arrows). Note that  $\kappa_{min}$  does not depend on the smoothing angle  $\theta_0$  but it depends on the background dynamics of the universe.

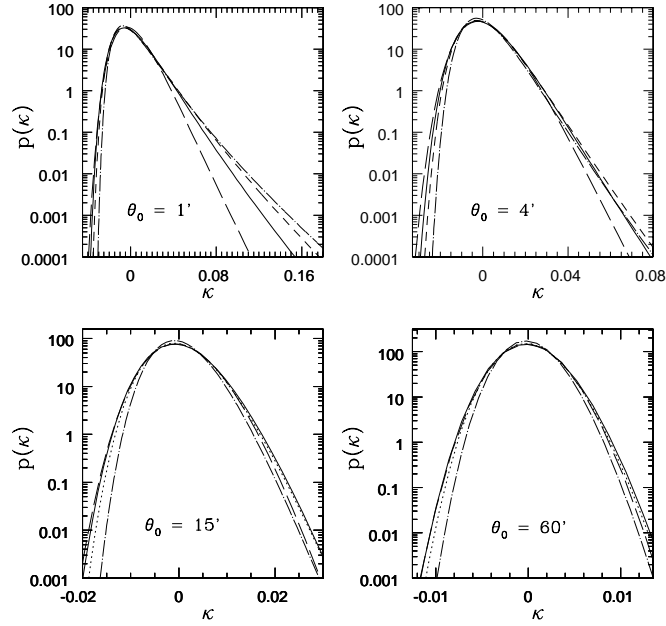


Fig. 2.— PDF associated with constant  $w_X$  models. Two different regimes are considered for computing the PDF. Upper panels  $\theta_s = 1', 4'$  correspond to the nonlinear calculations where we have assumed a hierarchical ansatz for the correlation hierarchy. For the lower panels perturbative results are used to construct the PDF at smoothing angles  $\theta_s = 15'$  and  $60'$ . Various curves correspond to various quintessence models. In each panel solid line represents the  $\Lambda$ CDM model, short dashed line represent  $w_X = -2/3$ , dot-dashed line represents  $w_X = -1/3$ , and long dashed line represents  $w_X = -1.9$ .

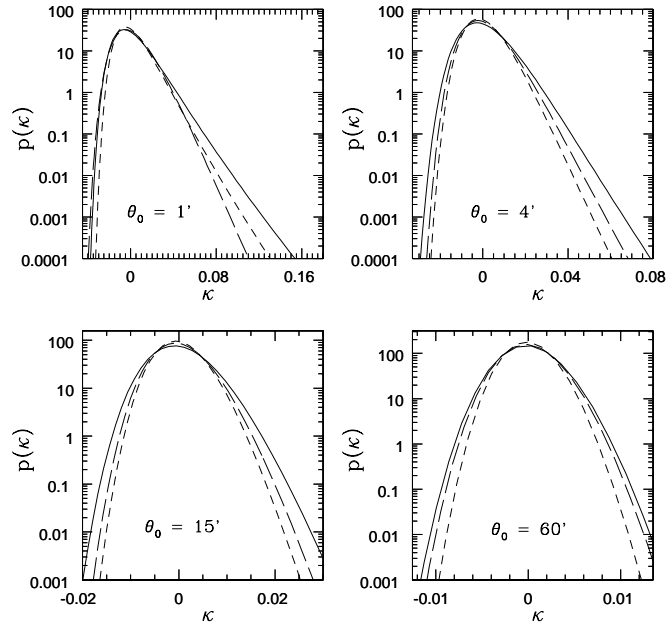


Fig. 3.— PDF associated with time-varying  $w_X$  models compared to  $\Lambda$ CDM. As in the previous figure two different regimes are considered for computing the PDF. Upper panels  $\theta_s = 1', 4'$  correspond to the nonlinear calculations where we have assumed a hierarchical ansatz for the correlation hierarchy. For the lower panels perturbative results are used to construct the PDF at smoothing angles  $\theta_s = 15'$  and  $60'$ . Various curves correspond to various quintessence models. In each panel solid line represents the  $\Lambda$ CDM model, short dashed line represent  $w_X = -1 + z$  model and long dashed line represents  $w_X = -1 + 2z/3$  model.

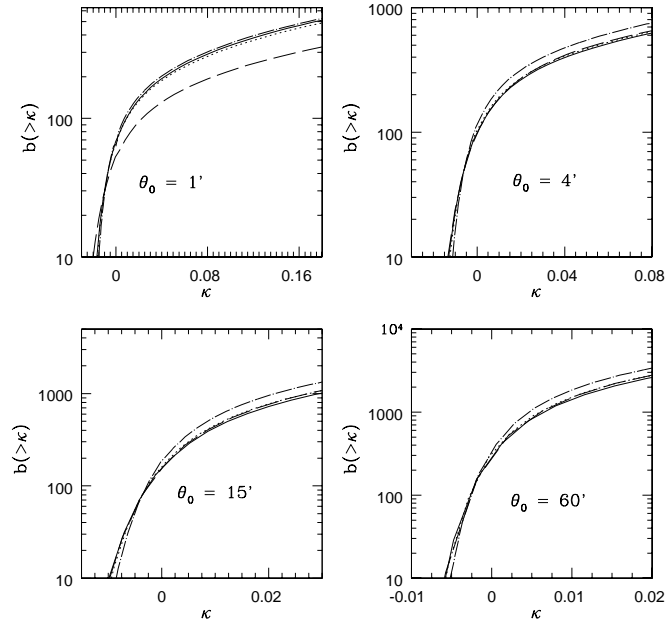


Fig. 4.— Bias associated with constant  $w_X$  models. Two different regimes are considered for computing the PDF. Upper panels  $\theta_s = 1', 4'$  correspond to the nonlinear calculations where we have assumed a hierarchical ansatz for the correlation hierarchy. For the lower panels perturbative results are used to construct the PDF at smoothing angles  $\theta_s = 15'$  and  $60'$ . Various curves correspond to various quintessence models. In each panel solid line represents the  $\Lambda$ CDM model, short dashed line represent  $w_X = -2/3$ , dot-dashed line represents  $w_X = -1/3$  and long dashed line represents  $w_X = -1.9$ .

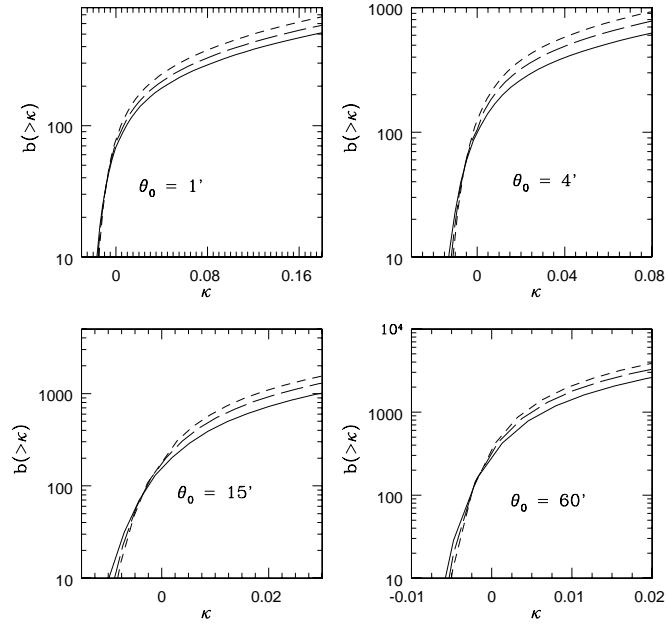


Fig. 5.— Bias associated with time-varying  $w_X$  models compared to  $\Lambda$ CDM. As in previous figure two different regimes are considered for computing the PDF. Upper panels  $\theta_s = 1', 4'$  correspond to the nonlinear calculations where we have assumed a hierarchical ansatz for the correlation hierarchy. For the lower panels perturbative results are used to construct the PDF at smoothing angles  $\theta_s = 15'$  and  $60'$ . Various curves correspond to various quintessence models. In each panel solid line represents the  $\Lambda$ CDM model, short dashed line represent  $w_X = -1 + z$  model and long dashed line represents  $w_X = -1 + 2z/3$  model.

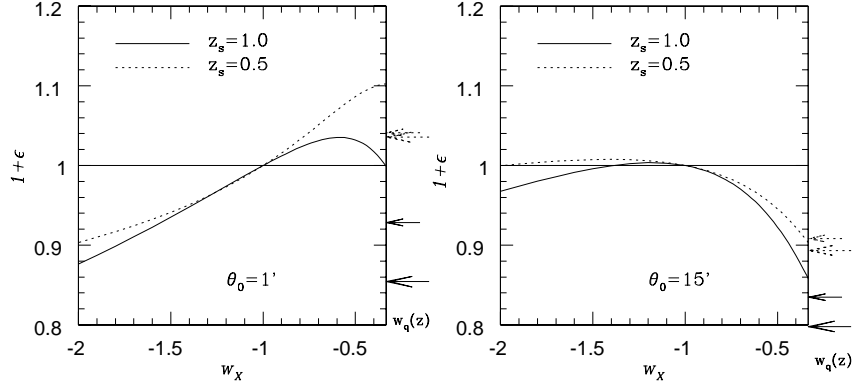


Fig. 6.— Indicator of the deviations of dark energy models from the fiducial  $\Lambda$ CDM model,  $1 + \epsilon$ , as function of constant dark energy equation of state  $w_X$ , for smoothing angle  $\theta_0 = 1'$  and  $15'$ . The arrows indicate the  $1 + \epsilon$  values for dark energy models with time-varying equation of state,  $w_q(z) = -1 + z$  (long arrows) and  $w_q(z) = -1 + 2z/3$  (short arrows).

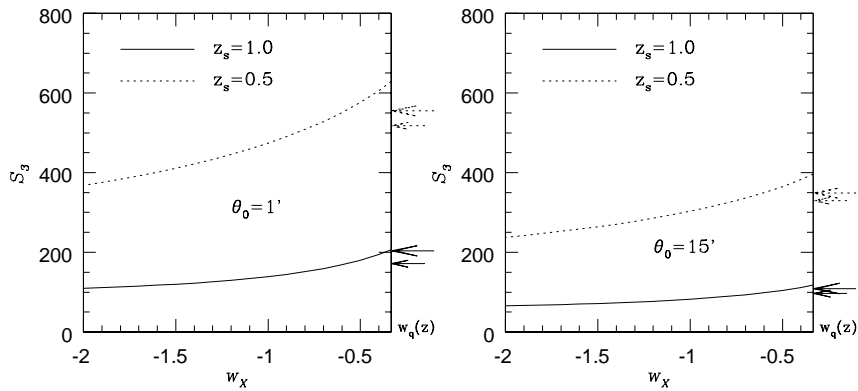


Fig. 7.— The skewness  $S_3$ , for the same models as in Fig.6. The line and arrow types are the same. In the left panel we use Hyper-Extended Perturbation theory to compute the convergence skewness, whereas in the right panel (where larger smoothing angular scales are considered) perturbative results are adopted.